ACS FOOD SCIENCE & TECHNOLOGY

pubs.acs.org/acsfoodscitech

Article

Cryo-Ground Mango Kernel Powder: Characterization, LC-MS/MS Profiling, Purification of Antioxidant-Rich Gallic Acid, and Molecular Docking Study of Its Major Polyphenols as Potential Inhibitors against SARS-CoV-2 M^{pro}

Bhupinder Kaur,* Himadri Sekhar Maity, Madhulekha Rakshit, Prem Prakash Srivastav, and Ahindra Nag

Cite This: https://doi.org/10.1021/acsfoodscitech.1c00179

Read Online

ACCESS | Metrics & More | Article Recommendations | Supporting Information

ABSTRACT: Mango processing waste (MPW) is an inexpensive and rich source of valuable substances. Hence, the mango kernel powder (MKP) from four cultivars (Chausa, Neelum, Barahmasi, and Dashehari) was characterized for the selection of the best cultivar. The MKP of the best cultivar (Dashehari) was analyzed for the profiling of polyphenols using LC-MS/MS in both modes of ionization (positive and negative) and indicated the presence of 50 compounds with specific retention times. After identification, gallic acid (GA), an important industrial compound, was targeted and purified followed by its confirmation using NMR (600 MHz) and HRMS. The antioxidant activity (IC_{50}: 1.96 μg/mL) of extracted GA proposes its use as a natural antioxidant in novel food formulations. Additionally, SARS-CoV-2 main protease (M^{pro}) was selected for molecular docking based virtual screening of seven major polyphenols (MKP), and the results were compared with hydroxychloroquine. The docking scores of targeted polyphenols revealed that three compounds (epicatechin, mangiferin, and quercetin) exhibited appreciable proteolytic activity against M^{pro}. In this way, it is a favorable approach toward environmental safety on the standpoint of green chemistry owing to the use of food processing waste and elimination of the waste dumping/composting problems.

KEYWORDS: *Mango kernel powder, Bioactive compounds, LC-MS/MS, Gallic acid, Molecular docking*

1. INTRODUCTION

The agricultural industries are responsible for generating millions of tons of byproducts at all stages of the supply chain, which are inexpensive and excellent sources of bioactive compounds.[1−4] If not processed, they can cause serious environmental issues such as pollution, combustion, vegetation damage, and greenhouse gas emission.[5] Moreover, byproducts can be utilized to and produce valuable products from their metabolites. The food processing waste can be utilized after valorization of valuable constituents, which in turn contributes to environmental safety.[6,7] The extraction of the beneficial compounds from these wastes can be a cost-effective approach, as an alternative to the expensive compounds.[8] However, the potential application of byproducts in food supplementation depends strongly on their various properties.

Mango (*Mangifera indica*) is recognized as a "superfruit" due to the presence of many promising functional ingredients and has more than 1500 varieties (India). In 2017−18, India was the largest producer (21.253 MT) of mangoes accounting for almost 40% of the total worldwide production of mango.[9] Industrial processing of mango juice, pickles, puree, and other products generates redundant byproducts representing 40−50% of the fruit weight. Mango seed is a single flat oblong that can be fibrous or hairy on the surface, depending on the cultivar. The kernel inside the seed represents 45−75% of the seed and about 20% of the whole fruit.[10] Though not utilized on a commercial basis due to the need for further processing, mango seeds are said to contain functional and health beneficial properties which can be utilized after profiling of their cultivars.[7,11] In contrast to the pulp, the mango kernel contains more polyphenols. Gómez-Caravaca et al.[12] observed that mango pulp had the lowest concentration of bound phenolic compounds with 2.51 mg/100 g d.w. as compared to that of peel and seed (33.69 and 41.71 mg/100 g d.w.). Moreover, the concentrations of phenolic compounds in the mango pulp was 4.6 times lower than that of mango kernels.[13] Furthermore, mango kernel has higher bioactive compounds than other commercially grown fruits like avocado, jackfruit, and tamarind kernels.[14] Although several studies[11,15−18] suggest the antioxidant, anticancer, antiproliferative, antimicrobial, and cytotoxic activities of mango polyphenols including gallic acid (GA), but the complete knowledge of molecular basis for their activity remains unknown. Though, there are two results of GA metabolism in the body; the first is conversion to nonpharmacological active compounds, and the second one is transformation into compounds which exhibit pharmacological activity after metabolism.[19,20] Being a histone

Received: May 19, 2021
Revised: September 9, 2021
Accepted: September 24, 2021

acetyltransferase inhibitor, GA could counteract amyloid-induced neurotoxicity by selectively suppressing NF-κB activation in the animal model of Alzheimer's disease.[21] In addition, García-Rivera et al.[22] showed that GA could regulate IκK/IκB/NF-κB, MAPK, and MEK1/p90RSK/MSK signaling pathways in MDA-MB231 breast cancer cells. It is also responsible for the inhibition of p300/CBP mediated p65 acetylation and subsequent IκB/NF-κB signal activation, which could reduce the expression of inflammatory mediators in A549 lung cancer cells.[23]

Recently, the novel coronavirus disease (COVID-19) has been spreading around the world causing the deaths of 222,000,588 people as of September 7, 2021 (https://www.worldometers.info/coronavirus/). The researchers are urgently looking for potential inhibitors to the main protease (Mpro) of severe acute respiratory syndrome coronavirus-2 (SARS-CoV-2) to tackle the pandemic.[24] Even though vaccination ensures the buildup of immunity, reoccurrence of coronavirus disease has been seen. Bioactive components from natural sources might enhance immunity and reduce the chance of the occurrence of this disease.[25] Thus, this calls for the need for predicting plausible drug candidates from natural sources to inhibit COVID-19 virus, and this could be explored using molecular docking.[26] Molecular docking is a technique for computer-aided drug design by docking a ligand with the receptor's active site. It describes the actual site of compound interaction and also reveals the names of amino acids involved in the interaction.[27] The docking method yields a scoring function that correctly ranks drug candidates and also can propose structural hypotheses of drug target binding sites.[28]

Grinding of agricultural produce is an old technique which involves frictional forces. The intensive use of energy causes heat generation when larger particles are fractured into smaller sizes. The increase in temperature is unfavorable for the aroma, flavor, phenolics, and overall quality of the final product.[7,29] According to Réblová,[30] the easily oxidizable phenolic acids (i.e., gallic, gentisic, protocatechuic, and caffeic) showed a decrease in antioxidant activity with increasing temperature (in comparison with activity at 90 °C) at a slower rate than the less oxidizable ones (i.e., syringic, ferulic, and sinapic acids, and especially vanillic acid). On the other hand, cryogenic grinding maintains the low-temperature environment owing to the use of liquid nitrogen and results in retention of valuable constituents.[31] The cryogenic liquid absorbs the heat which is being generated due to frictional forces during grinding and helps to preserve the wholesomeness of the final product.

There are few studies on the phenolic composition of mango kernel powders obtained by regular grinding techniques.[32−36] However, a detailed literature review has shown that cryo-ground MKP has not yet been characterized. Hence, this study was proposed to elucidate the chemical, morphological, and phytochemical profiling of cryo-ground MKP along with isolation of antioxidant-rich gallic acid. In addition, major polyphenols derived from MKP were scrutinized for their potential interactions with SARS-CoV-2 M^{pro}. In this way, the industries can earn profit by cutting the transportation and dumping cost of waste. This would not only bring in extra revenue for the producer but also reduce the amount of accumulated waste to be disposed of.

2. MATERIALS AND METHODS

2.1. Raw Materials. The mango kernels of four cultivars (Chausa, Neelum, Barahmasi, and Dashehari) were collected during May−July 2017, from SRP Nutriment Pvt. Ltd., IIT Kharagpur (located at a latitude of 22.3145°N and longitude of 87.3091°E), West Bengal, India.

Sulfuric acid, sodium hydroxide, boric acid, Folin−Ciocalteu reagent, sodium carbonate, gallic acid aluminum chloride, sodium hydroxide, rutin, quercetin, 2,2-diphenyl-1-picrylhydrazyl (DPPH), ethanol (HPLC grade), formic acid, acetonitrile (HPLC grade), acetone, silica gel (60−120 mesh), TLC plates (Merck $60F_{254}$), ethyl acetate, hexane, DMSO-d_6, and $CDCl_3$ purchased from SRL (Sisco Research Laboratories) Chemicals, India, were used for the study.

2.2. Preparation of Mango Kernel Powder. The mango seeds were cracked using a nut shelling unit to obtain kernels and subjected to tray dryer (50 ± 3 °C) for 48 h. The grinding operation was carried out in cryogenic ball mill along with liquid nitrogen as cryogenic liquid (bp −196.5 °C). Our previous study[7] parameters for cryogenic grinding were used to acquire cryo-ground MKP. The obtained samples were sieved using a sieve shaker (Retsch GmbH, Haan, Germany) by passing through a set of standard sieves (710, 500, 300, 250, 212, 180, and 150 μm). The MKP (150 μm) samples were packed in airproof containers and stored in a refrigerator (4 ± 2 °C) for further analysis.

2.3. Characterization of Mango Kernel Powder. *2.3.1. Proximate Analysis of Mango Kernel Powder.* Moisture content was analyzed by using a digital Halogen moisture meter. The analysis of protein (Kjeldahl method), fat (Soxhlet extraction), crude fiber, and ash content of all samples were examined according to standard of Association of Official Analytical Chemists.[37] The carbohydrate content is determined as total Carbohydrate by difference.[7]

2.3.2. Mango Kernel Extract and Its Total Phenolic Content (TPC), Total Flavonoid Content (TFC), and Antioxidant Activity. Mango kernel extracts (MKE) of different cultivars were obtained by conventional extraction method. Ethanol was used as the extraction solvent as it is food grade in nature, as declared by US Food and Drug Administration (Bartnick, Mohler, & Houlihan 2006). MKP (1 g) mixed with ethanol (100 mL) was subjected to homogenization (hand-held minihomogenizer: MT-13K) for 10 min and the obtained suspension was kept in a water bath (45 °C) for 60−120 min; afterward it was centrifuged at 8000 *g* for 20 min^3 followed by filtration through filter paper (Whatman No. 4). After filtration, the clear extract was examined for total phenolics, total flavonoids, and antioxidant activity.[38]

2.3.3. Microstructure and Mineral Analysis of Mango Kernel Powder. The samples were made conductive by gold coating before their introduction to the SEM characterization cell. The Merlin SEM-EDX (scanning electron microscopy with energy-dispersive X-ray spectroscopy), based on the GEMINI II column (Carl Zeiss, Merlin FE-SEM, Oberkochen, Germany), examined the shape, geometry, and mineral profile. The instrument was coupled with ZeissSmartSEM and INCA PentaFET × 3 (Oxford Instrument, High Wycombe, UK) analysis software. The study was carried out in three iterations.

2.4. Identification of Polyphenols Using LC-MS/MS. The identification of polyphenols was carried out using an LC-MS/MS Waters 2695 separation module (Waters, USA) interfaced with Micromass Quattro Micro Triple Quadrupole mass spectrometer (Micromass, Manchester, UK) with MassLynx 4.1 software.[39]

2.4.1. Chromatographic Conditions. The gradient elution ((0.1% aq. formic acid (A) and acetonitrile (B)) was carried out using XTerra MS C18 reversed phase column (2.1 × 100 mm, 2.5 μm, Waters) operated at 25 °C. The elution gradient of 15−45% (B) in 0−25 min and 45−70% (B) in 25−35 min and initial condition with 0.4 mL/min flow rate was maintained for 5 min. The sample at a flow rate of 0.8 mL/min was infused into the electropray ionization source using the syringe pump. The MSKE (10 μL) was filtered through 0.45 μm membrane syringe filter prior to injection.

2.4.2. MS Operating Conditions. The MS was operated in both negative and positive ion mode with capillary voltage of 3 kV and cone voltage 30 V. The spectrum of the column eluate was acquired in the scan range of 50−1000 (m/z); the scan time and interscan delay time were 0.5 and 0.1 s, respectively. Nitrogen was used as drying, nebulizing, and collision gas. The heated capillary temperature was set at 350 °C and nebulizer pressure at 45 psi. An electrospray source block temperature 130 °C and desolvation temperature 300 °C were used.

https://doi.org/10.1021/acsfoodscitech.1c00179
ACS Food Sci. Technol. XXXX, XXX, XXX−XXX

Table 1. Proximate and Phytochemical Composition of Cryo-Ground MSKP from Different Cultivars (n = 4)[a]

cultivar	moisture content (%)	ash (%)	fat (%)	protein (%)	dry extract yield (g/100 g DW)	TFC (mg QE/g)	TPC (mg GAE/g)	IC_{50} (μg/mL)
Chausa	9.29 ± 0.011^{b}	2.20 ± 0.035^{a}	8.83 ± 0.207^{a}	6.02 ± 0.214^{a}	8.35 ± 0.122^{c}	73.3 ± 0.006^{d}	25.8 ± 0.193^{e}	24.86 ± 0.018^{c}
Neelum	9.54 ± 0.012^{ab}	2.13 ± 0.025^{a}	6.79 ± 0.125^{d}	5.49 ± 0.141^{b}	7.58 ± 0.111^{d}	111.8 ± 0.008^{c}	36.5 ± 1.023^{d}	31.56 ± 0.094^{b}
BarahMasi	9.52 ± 0.007^{ab}	1.54 ± 0.036^{d}	7.61 ± 0.065^{c}	6.01 ± 0.104^{a}	7.74 ± 0.087^{d}	169.3 ± 0.112^{a}	49.9 ± 0.052^{b}	21.40 ± 0.143^{d}
Dashehari	8.13 ± 0.010^{c}	1.65 ± 0.055^{c}	6.58 ± 0.227^{d}	5.60 ± 0.117^{b}	10.33 ± 0.092^{a}	169.4 ± 0.024^{a}	52.4 ± 0.104^{a}	34.95 ± 0.131^{a}

[a]Results are expressed as mean ± SD of triplicates. SD followed by different letter superscripts within each column is significantly different ($P \leq 0.05$).

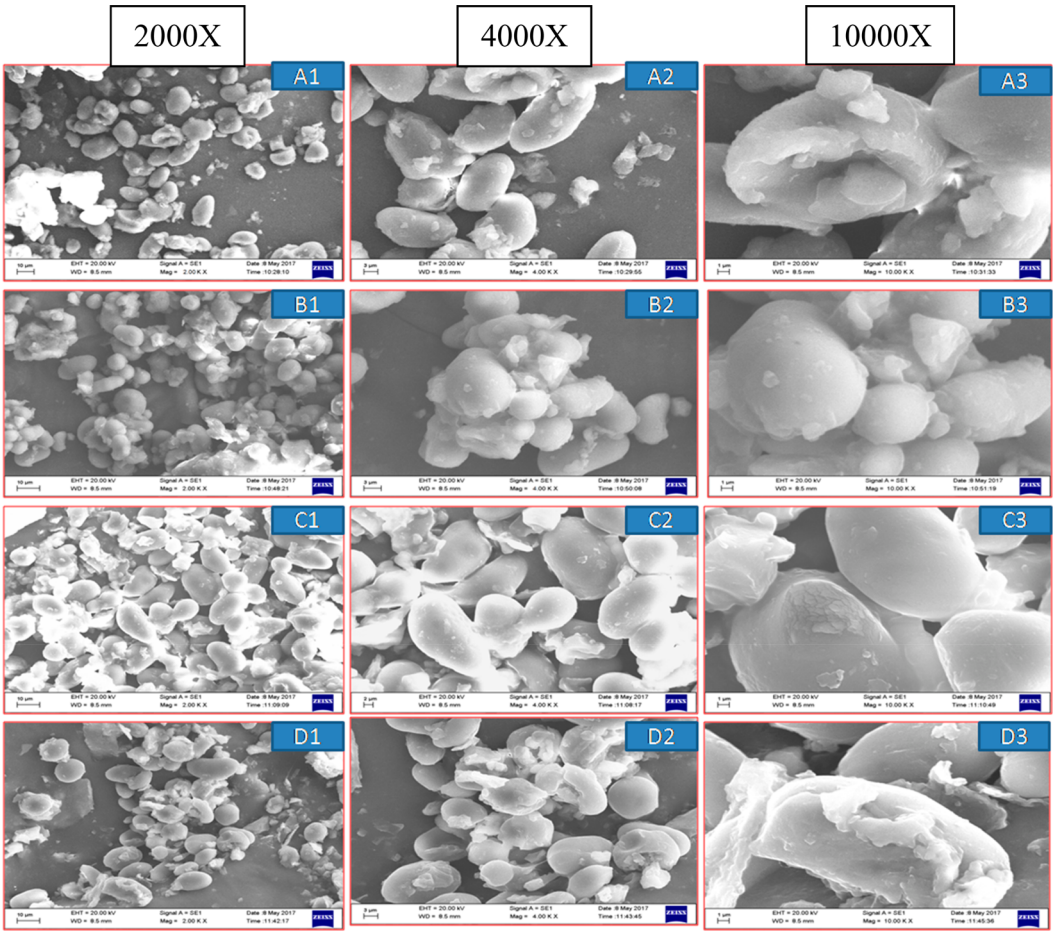

Figure 1. SEM micrographs of cryo-ground mango seed kernel powder from different cultivars (n = 4), i.e., [A1−A3] Chausa; [B1−B3] Neelum; [C1−C3] Barahmasi; [D1−D3] Dashehari.

For the MS/MS analysis, argon gas with collision energy of 30 eV was employed to fragment bioactive compounds. The analysis was carried out in three iterations.

2.5. Purification of Gallic Acid Using Column Chromatography. The ethanolic MSKE was at first dried over anhydrous sodium sulfate, and the solvent was evaporated to dryness. The crude residue was purified by flash column chromatography on silica gel (60−120 mesh). The mobile phase of ethyl acetate:hexane (EtOAc:Hx) was optimized with different proportions (0−100% (v/v)) for the fractionation. The effluent from the outlet of the column was collected in test tubes and analyzed using TLC plate (Merck $60F_{254}$). The TLC plates were continuously monitored with a UV detector and mixed according to their purity. The fractions containing GA were mixed together and evaporated to dryness for rechromatography on silica gel (230−400 mesh). The purified GA was then quantified and further analyzed by NMR (600 MHz) and HRMS for structural confirmation.

2.6. Confirmation of Purified Gallic Acid by NMR and HRMS. The NMR spectroscopic data was obtained using a Bruker Avance DPX200 (600 MHz) instrument along with trimethylsilane (TMS) as internal reference. ^{1}H NMR and ^{13}C NMR spectra were recorded via broadband decoupled mode at 600 and 150 MHz, respectively. The solvent used was DMSO-d_6 with proton and carbon shifts as δ 2.50 and 39.52 ppm, respectively. The compound concentration used for analysis was 20 mg/mL.

The high resolution mass spectrometer (HRMS) of Agilent 1260 Infinity II coupled with AdvanceBIO 6545XT LC/Q-TOF was used to confirm the mass of purified gallic acid.

2.7. DPPH Scavenging Activity of Purified Gallic Acid. The antioxidant activity of isolated GA was determined according to Rafiee et al.[40] and compared with rutin and quercetin with slight modification.

2.8. Molecular Docking Studies of Major Polyphenols of MSK against SARS CoV-2 M^{pro}. The RCSB Protein Data Bank (http://www.rcsb.org) (PDB ID: 6Y2F) was referred for obtaining the crystal structure of the SARS CoV-2 main protease,[41] and the ligands were obtained from PubChem (https://pubchem.ncbi.nlm.nih.gov) database. The docking of the main protease with seven polyphenols of mango was conducted by using AutoDock Vina software. The binding energies of M^{pro} and selected compounds were evaluated using the

https://doi.org/10.1021/acsfoodscitech.1c00179
ACS Food Sci. Technol. XXXX, XXX, XXX−XXX

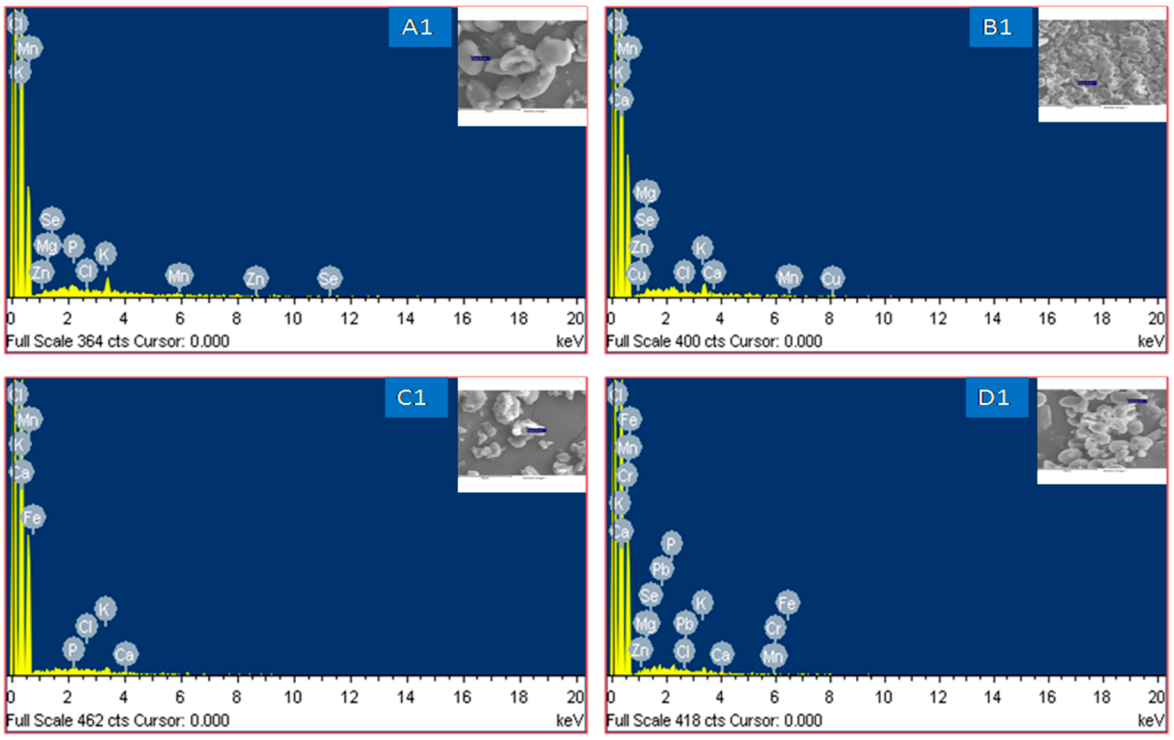

Figure 2. SEM-EDX spectrum of cryo-ground mango seed kernel powder from different cultivars (n = 4), i.e., [A1] Chausa; [B1] Neelum; [C1] Barahmasi; [D1] Dashehari.

same software. The dimensions grid-box generated was 5 Å × 5 Å × 5 Å at *X*, 6.852; *Y*, 0.154; *Z*, 18.885 so as to fit all the ligands. The output from AutoDock Vina was visualized with Discovery studio 2020.

2.9. Statistical Analysis. SPSS (Version 20.0, IBM Corporation, USA) software was employed for statistical study. The significance of variables was determined by One-Way ANOVA. The mean comparison was done by Post Hoc Duncan's multiple range test and significantly different means were denoted with (a−d) subscripts. All findings were expressed as mean ± SD (standard deviation).

3. RESULTS AND DISCUSSION

3.1. Characterization of Mango Kernel Powder. *3.1.1. Proximate Analysis of Mango Kernel Powder.* MKP has an impressive amount of essential nutrients, minerals, phenolics, and flavonoids required for human well-being. The moisture content of any powdered material is a critical parameter for its life span.

The moisture content of all the varieties ranged from 8.13 ± 0.010% to 9.54 ± 0.012% (Table 1) which is bit higher than other powdered food products. So, they were properly stored in airtight containers. Chausa (2.20 ± 0.035%) and Neelum (2.13 ± 0.025%) had high ash content with an insignificant difference, which gives an indication of the minerals present in it. They play a very important role in biochemical reactions as catalyst (metalloenzyme), which helps to maintain the body's metabolism. The main attraction of mango waste is mango kernel oil (MKO), and Chausa (8.83 ± 0.207%) had the highest fat content among all the varieties, which can be utilized in chocolates as a cocoa butter substitute.[2]

3.1.2. Phytochemical Profile of Mango Kernel Extract. Mango kernel is a rich source of polyphenols, viz., phenolic acids, lignans, stilbenes, and flavonoids. The data for yield, TPC, TFC, and antioxidant activity (IC_{50}) in the MSK of four cultivars is expressed in Table 1. The yield of total polyphenols from ethanolic MSKE was observed as (7.58 ± 0.111)−(10.33 ± 0.092) g/100 g d.w., which is higher than that of mango peel and seed dehydrated by various drying treatments and Egyptian mango cultivars.[4,34] The probable reason for higher values could be environmental factors and cryogenic grinding that helps to preserve the beneficial heat-sensitive compounds. The samples contained much higher total flavonoids than total phenolics, ranging from 73.3 ± 0.006 to 169.4 ± 0.024 mg QE/g, the highest levels being present in Dashehari and Barahmasi (169.4 ± 0.024 and 169.3 ± 0.112 mg QE, respectively).

The findings of Ajila et al.[42] explored that bound phenolics in mango peel (ripen) dietary fiber from both Raspuri (29.52 ± 1.73 mg GAE/g) and Badami (28.10 ± 0.10 mg GAE/g) cultivar were comparable to the data of present study. Among all the cultivars, the lowest TPC value of Chausa (25.8 ± 0.193 mg GAE/g) was closer to the highest values reported by Tunchaiyaphum et al.[43] The papaya seed [(8.55 ± 0.49)−(22.59 ± 0.06 mg) GAE/g] and MKP from Egyptian cultivar named Zebda (23.90 ± 0.33 mg GAE/g) showed lower TPC values.[35,44]

The IC_{50} value was calculated from a linear regression equation to range between 21.40 ± 0.143 and 34.95 ± 0.131 μg/mL (R^2 = 0.97). The IC_{50} is inversely proportional to the antioxidant activity. The Barahmasi cultivar exhibited the highest antioxidant activity (IC_{50}: 21.40 ± 0.143 μg/mL). The antioxidant activities of MSKE were higher than those of standard BHT and tocopherol, respectively.[36,45] Comparing our previous results of mango peel powder[7] with our present results, the MKP explored that both the total flavonoid and total phenolic contents are higher in the seed as compared to the peel, while there was not much difference observed in IC_{50} values for all the cultivars.

3.1.3. Microstructure of Mango Kernel Powder. SEM with a wide range of resolution was used to visualize the internal geometry and surface morphology of MKP. The typical

https://doi.org/10.1021/acsfoodscitech.1c00179
ACS Food Sci. Technol. XXXX, XXX, XXX−XXX

Table 2. LC-MS/MS Profile of Bioactive Compounds in Mango Kernel Extract

sample no.	RT (min)	precursor ion [M-H]	diagnostic fragments	molecular formula	molecular weight (g/mol)	compound Identified
1	1.16	191	173, 111	$C_6H_8O_7$	192.12	Citric acid
2	1.97	148	103	$C_9H_8O_2$	148.15	Cinnamic acid
3	2.05	163	241, 119	$C_9H_8O_3$	164.16	*p*-Coumaric acid
4	2.41	133	115	$C_4H_6O_5$	134.09	Malic acid
5	2.76	169	125	$C_7H_6O_5$	170.12	Gallic acid
6	3.34	331	330, 211, 169, 125	$C_{13}H_{16}O_{10}$	332.26	*β*-Glucogallin
7	3.42	493	312	$C_{19}H_{26}O_{15}$	494.40	Gallic acid dihexose
8	4.29	249	133, 114	$C_8H_{10}O_9$	250.16	Oxydisuccinic acid
9	4.63	190	172, 125, 109	$C_7H_{12}O_6$	192.17	Quinic acid
10	4.81	179	135	$C_9H_8O_4$	180.16	Caffeic acid
11	6.05	421	331, 301, 271, 258	$C_{19}H_{18}O_{11}$	422.33	Mangiferin
12	6.38	331	271, 211, 169	$C_{13}H_{16}O_{10}$	332.26	Galloylhexose
13	7.19	289	285, 205, 151, 125	$C_{15}H_{14}O_6$	290.26	(+)-Catechin
14	8.04	300	283, 228, 200, 172, 145, 117	$C_{14}H_6O_8$	302.20	Ellagic acid
15	9.11	197	169, 125	$C_9H_{10}O_5$	198.17	Ethyl gallate
16	10.54	635	331,301, 270, 211, 169	$C_{27}H_{24}O_{18}$	636.5	Trigalloylglucose
17	10.65	182	169, 125	$C_8H_8O_5$	184.15	Methyl gallate
18	11.08	463	300, 299, 283, 257	$C_{20}H_{16}O_{13}$	464.33	Ellagic acid-*O*-hexoside
19	11.20	285	227, 211	$C_{15}H_{10}O_6$	286.23	Kaempferol
20	12.63	305	273, 174, 146	$C_{14}H_{10}O_8$	306.22	Methyl brevifolincarboxylate
21	13.75	353	191	$C_{16}H_{18}O_9$	354.31	Chlorogenic acid
22	14.63	609	301	$C_{27}H_{30}O_{16}$	610.52	Rutin
23	14.87	343	179	$C_{15}H_{18}O_9$	342.3	Caffeoyl glucose
24	15.01	463	301, 300, 270, 255	$C_{21}H_{20}O_{12}$	464.09	Quercetin-*O*-hexoside
25	15.16	325	163, 119	$C_{15}H_{18}O_8$	326.3	Coumaryl-hexoside
26	15.74	289	245, 202,161	$C_{15}H_{14}O_6$	290.26	Epicatechin
27	16.12	331	315, 314, 299, 270	$C_{16}H_{10}O_8$	330.25	Dimethyl-*O*-ellagic acid
28	17.49	595	300, 301, 270	$C_{26}H_{28}O_{16}$	596.5	Quercetin-3-sambubioside
29	18.36	593	285, 227	$C_{27}H_{30}O_{15}$	594.52	Kaempferol-3-*O*-rutinoside
30	18.42	317	299	$C_{15}H_8O_8$	316.22	Methy-*O*-ellagic acid
31	18.57	517	353, 191	$C_{25}H_{24}O_{12}$	516.45	1,3-Dicaffeoylquinic acid
32	19.22	517	516, 191	$C_{25}H_{24}O_{12}$	516.45	4,5-Dicaffeoylquinic acid
33	19.79	461	285, 255	$C_{21}H_{18}O_{12}$	462.36	Luteolin-7-*O*-glucuronide
34	19.90	483	330, 271, 211, 169	$C_{20}H_{20}O_{14}$	484.4	Digalloylglucose
35	20.44	594	285, 255	$C_{27}H_{32}O_{15}$	596.53	Luteolin-4′-*O*-rutinoside
36	20.81	483	330, 312, 169	$C_{20}H_{20}O_{14}$	484.36	Digalloyl-hexoside
37	21.63	301	270, 257	$C_{15}H_{10}O_7$	302.24	Quercetin
38	21.74	353	191, 173, 109	$C_{16}H_{18}O_9$	354.31	1-Caffeoylquinic acid
39	22.58	193	178, 135	$C_{10}H_{10}O_4$	194.18	Ferulic acid
40	22.31	771	153	$C_{34}H_{26}O_{21}$	770.56	Di-*O*-galloyl-2,3-(*S*)-hexahydroxydiphenoyl-scyllo-quercitol
41	23.11	787	634, 617, 573, 483, 464, 169	$C_{34}H_{28}O_{22}$	788.58	Tetragalloylglucose
42	23.20	786	634, 301	$C_{34}H_{26}O_{22}$	786.56	Digalloyl-HHDP-glucose
43	24.92	545	768, 392, 317, 169	$C_{24}H_{18}O_{15}$	546.39	Dihydroxybenzoicacetate-digallate III
44	25.59	808	463, 300	$C_{33}H_{28}O_{24}$	808.58	Mallonin
45	26.24	453	307	$C_{30}H_{48}O_3$	456.7	Oleanolic acid
46	27.16	343	313, 298	$C_{18}H_{16}O_7$	344.32	Nevadensin
47	28.63	313	298	$C_{17}H_{14}O_6$	314.29	Cirsimaritin
48	30.42	939	787, 769, 617	$C_{41}H_{32}O_{26}$	940.67	Pentagalloylglucose
49	30.95	634	463, 301	$C_{27}H_{22}O_{18}$	634.45	Galloyl-HHDP-glucose
50	31.68	938	634, 468, 301	$C_{41}H_{30}O_{26}$	938.66	Trigalloyl-HHDP-glucose

microstructure of cryo-ground mango kernel particles is shown in Figure 1 at different magnifications, i.e., 2000×, 4000×, 10,000×.

The microstructure of mango kernel changed during grinding operation, which could have a significant impact on physicochemical, functional, and rheological properties. During the transformation of an ordered to a disordered structure, there is breakage of bonds.[46] For all the cultivars, smooth, oval, and irregularly shaped particles can be clearly seen at all magnifications. The micrographs of cryogenic fracture surfaces of Dashehari at 2000× and 4000× showed the lumpy structure. This might be due to its high moisture content. At 10,000×, the

https://doi.org/10.1021/acsfoodscitech.1c00179
ACS Food Sci. Technol. XXXX, XXX, XXX−XXX

Table 3. ^{1}H NMR and ^{13}C NMR Data of Purified Gallic Acid Using DMSO-d_6 as Solvent[a]

Position	Experimental δ_H (ppm)	*Reported δ_H (ppm)	Experimental δ_C (ppm)	**Reported δ_C (ppm)	Gallic acid structure
1 and 5	6.91	6.91	109.07	108.14	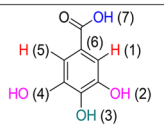
2 and 4	9.18	9.19	145.77	143.98	
3	8.84	8.85	138.35	136.61	
6	-	-	120.80	119.87	
7	12.24	12.24	167.84	167.01	

[a]*δ_H: Lopez-Martinez et al.[38] **δ_C:Kamatham et al.[39]

particles of all cultivars can be seen packed closely, which indicates their poor flowability. The combination of high mechanical impact force and attrition produced small-sized particles, some of which contributes to amorphous domain. It can be said that cryogenic grinding was effective at altering the actual shape and structure of the MSK. The biological origin, varietal difference, maturity index, and physiology are the possible reasons for variation in size and shape of all the samples.

3.1.4. Mineral Profile of Mango Kernel Powder. The mineral profile indicated the amount of inorganic matter present in the sample. The SEM-EDX was used, and particular areas were focused to obtain the spectrum (Figure 2). Potassium, calcium, manganese, and chlorine were observed as highlighted peaks in almost all the cultivars. Among all the cultivars, only Chausa was revealed to have sodium which helps to maintain the acid−base balance. It also had the highest calcium (21.49 ± 0.02%) which is a component of bones and teeth; additionally, it plays an important role in muscle contraction and blood clot-related mechanisms.

Although Barahmasi (MKP) does not contain many minerals, it has significant amounts of phosphorus (8.83 ± 0.06%), potassium (63.51 ± 0.017%), and iron (13.87 ± 0.05%), which aid in formation of healthy teeth and bones, maintain fluid balance, and help in functioning of the central nervous system (CNS), respectively (SI Table 1). Among all observed minerals, potassium was the dominant element in mango peel and pulp.[7,47]

These finding are in line with the study undertaken for Barahmasi (MKP) that also showed potassium (63.51 ± 0.017%) as the highlighted element. This Na−K interaction helps in nerve transmission and muscle contraction/relaxation. The ratio of potassium to sodium content is very much important, especially considered for patients with high blood pressure.

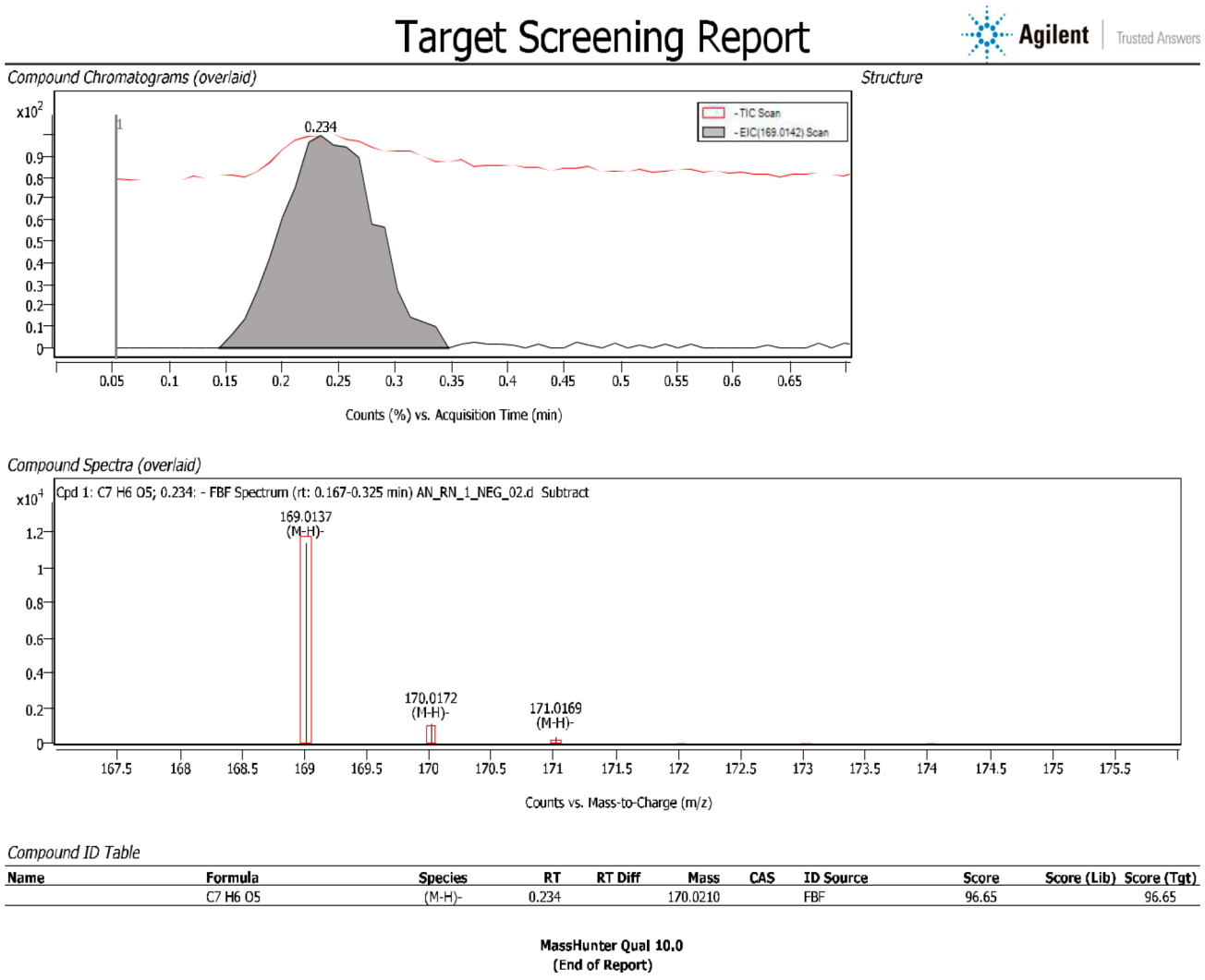

Figure 3. HRMS chromatogram of gallic acid obtained after column chromatography.

https://doi.org/10.1021/acsfoodscitech.1c00179
ACS Food Sci. Technol. XXXX, XXX, XXX−XXX

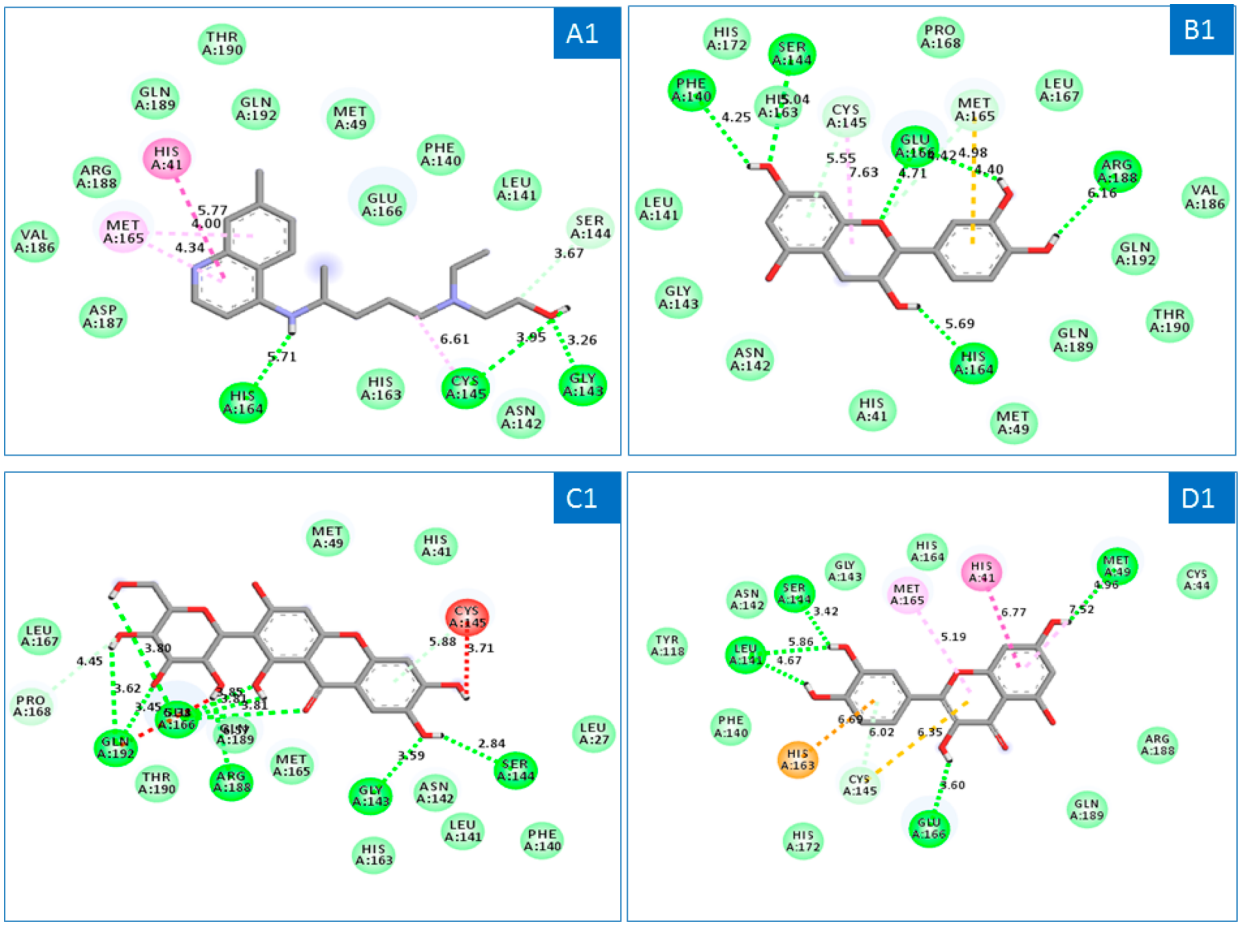

Figure 4. 2D ligand interaction diagram showing the interactions of (A1), Hydroxychloroquine; (B1), epicatechin; (C1), mangiferin; and (D1), quercetin and active site residues of M^{pro}.

3.2. Identification of Bioactive Compounds Using LC-MS/MS. The results obtained from phytochemical analysis (Table 1) revealed that the Dashehari cultivar exhibited the highest values of TPC and TFC. Hence, the Dashehari variety was selected for further identification of bioactive compounds using LC-MS/MS.

The LC-MS analysis was carried out in both ionization modes to obtain protonated/deprotonated molecules (SI Figure 1(a, b, c, d, e, f)). However, the negative mode was more favorable for the detection of phenolic compounds due to their acidic behavior. The retention time, precursor ion, diagnostic fragments, molecular formula, molecular weight, and tentative identification of compounds is summarized in Table 2. The retention time and fragmentation data of available standards were used to confirm a compound. Despite the lack of authentic standards, very reliable and tentative identification of 50 compounds was proposed by comparing the obtained fragmentation patterns with previously reported daughter ions in the literature.

During the initial run time of 1−5 min, organic acids, viz., citric acid, cinnamic acid, malic acid, gallic acid, and quinic acid (**1**, **2**, **4**, **5**, and **9**) were explored. MS/MS spectra of compounds **2**, **4**, and **5** showed fragment ions at m/z 103, 115, and 125, respectively. Fruits are a rich source of citric acid (**1**) and hydroxycinnamic acids (**3**, **10**, **21**, and **39**); moreover, many researchers have reported their potential as strong antioxidant agents.[48] Compound **3** was tentatively assigned as a *p*-coumaric acid which presented fragments at m/z 241 and 119 due to the loss of CO_2 from the carboxylic group. Caffeic acid (**10**) and chlorogenic acid (**21**) yielded minor ions at m/z 135 and m/z 191, which correspond to elimination of CO_2 and deprotonated quinic acid, respectively. Compound **39** was designated as ferulic acid,[49] which produced fragment ions due to cleavage of the methyl group (m/z 178) and sequential loss of CO_2 (m/z 135). Compound **4** was identified in the negative mode at m/z 133 with fragment ion at m/z 115 corresponding to the malic acid fragmentation pattern.

Compounds **5** and **9** were assigned as gallic acid (SI Figure 2) and quinic acid with their base peak at m/z 125 due to loss of CO_2. The MS data of these compounds were also matched with commercial standards.

Mangiferin (**11**) was identified in both negative and positive ion modes with major ions at m/z 423/421 along with daughter ions at m/z 331 (90 Da) and 301 (120 Da) indicating the loss of C-glycoside xanthone. (+)-Catechin (**13**), a flavan-3-ol, produced the product ions at m/z 285 and 151 due to loss of sugar moiety and CH_3.[38] The precursor ion at m/z 289 produced the product ions at m/z 245, 202, and 161. Such a fragmentation pattern confirmed the presence of another flavan-3-ol compound **26** (Epicatechin). Caffeoyl glucose (**23**) showed a pseudomolecular ion at m/z 343 and characteristic fragment ion at m/z 179 (Caffeic acid). In positive ionization mode, compounds **31** and **32** showed a pseudomolecular ion at m/z 517 with base peak at m/z 191 corresponding to quinic acid in structure. These compounds were identified as 1,3-dicaffeoylquinic acid (**31**) and 4,5-dicaffeoylquinic acid (**32**), based on the

https://doi.org/10.1021/acsfoodscitech.1c00179
ACS Food Sci. Technol. XXXX, XXX, XXX−XXX

obtained MS data and the literature.[50] The deprotonated ion peak at m/z 353 for compound **38** (RT 21.74) showed product ions at m/z 191, 173, and 109 and was characterized as 1-aaffeoylquinic acid.[51]

Quercetin was assigned to compound **37** (RT 21.63 min) with the precursor ion at m/z 301; additional confirmation was done by comparison of their mass fragments with standard compound and previously published data. Two compounds at 11.08 and 15.01 min exhibited the same precursor ion at m/z 463 and common fragment at m/z 300 confirming the elimination of the hexoside moiety. Additionally, compound **18** (ellagic acid-*O*-hexoside) gave minor ions at m/z 283 and 257 corresponding to the loss of H_2O and 2CO. In contrast, compounds **22** and **24** fragmented at m/z 301, suggesting the presence of Quercetin derivatives and tentatively acknowledged as qutin and quercetin-*O*-hexoside, respectively.[52] Compound **25** (coumaryl-hexoside) showed minor ions at m/z 163 (*p*-coumaric acid) and 119 due to removal of CO_2 from carboxylic group.[53]

Two flavone derivatives **33** and **35** were tentatively characterized as luteolin-7-*O*-glucuronide and luteolin-4′-*O*-rutinoside with a common fragment obtained at m/z 285 and 255, corresponding to the loss of sugar moiety and CHO, respectively. Moreover, the methoxy-substituted flavones comprising nevadensin and cirsimaritin, which were not the focus of the present work, were confirmed by matching the fragments with Ola et al.[54] Compound **14** had a molecular weight of 302 and showed fragment ions at m/z 283, 172, and 145 due to the loss of H_2O, the presence of the shikimate moiety, and the loss of a neutral alkyl moiety, respectively. The structure was unambiguously identified as ellagic acid and increased the probability of identifying its derivatives. Dimethyl-*O*-ellagic acid (**27**) and methy-*O*-ellagic acid (**30**) showed characteristic fragment ions at m/z 314 and 299, respectively, due to the elimination of CH_3.[49] The pseudomolecular ion at m/z 285 gave product ions at m/z 227 owing to the loss of 2CHO and assigned as kaempferol (**19**). Moreover, another compound (**29**: kaempferol-3-*O*-rutinoside) explored a daughter ion at m/z 285 (kaempferol) and 227 corresponding to the loss of *O*-hexoside and 2CHO. The fragment of compound **20** at m/z 273 resulted from the elimination of CH_3OH; such results confirm the presence of methyl brevifolincarboxylate, and compound **45** was confirmed as oleanolic acid by comparison of RT and fragmentation patterns with those reported by Kumar et al.[49]

Nine compounds (**6**, **12**, **15**, **16**, **17**, **34**, **36**, **41**, and **43**) displayed fragment ions at m/z 169 (Table 2) as a consequence of losing gallate. According to their fragmentation, the tentatively identified compounds were *β*-glucogallin (**6**), galloylhexose (**12**), ethyl gallate (**15**), trigalloylglucose (**16**), methyl gallate (**17**), digalloylglucose (**34**), digalloyl-hexoside (**36**), tetragalloylglucose (**41**), and dihydroxybenzoicacetate-digallate III (**43**). Moreover, compounds **15** and **17** showed base peak at m/z 125 and produced the product ion at m/z 169 (gallic acid) due to loss of C_2H_5 and CH_3, respectively. Three compounds (**50**, **42**, and **49**) exhibited pseudomolecular ions at m/z 938/786/634 with common daughter ions at m/z 301 (loss of HHDP-glu). These fragmentation patterns were identical to trigalloyl-HHDP-glucose, digalloyl-HHDP-glucose, and galloyl-HHDP-glucose, as reported by Yang et al.[55] Compound **48** (m/z 939) gave fragments at m/z 787 (152 Da: loss of galloyl unit) and 769 (170 Da: loss of gallic acid), which is the typical fragmentation pattern of pentagalloylglucose.[56]

3.3. Purification of Gallic Acid by Column Chromatography. Initially, the column was run with hexane in order to remove the fatty part to avoid the isolation complexity of polar compounds. The MKE was separated into nine fractions (F_{1-9}) according to the polarity. All the fractions were monitored against standard GA for their purity using TLC. The fractions resulted into mixture (impure) of compounds as it was observed that chromatogram (TLC) showed more than one band under UV lamp (SI Figure 3(a, b, c)). F_{6-9} were discarded because they showed no traces of gallic acid. However, F_{2-4} contained GA along with other compounds, so they were combined for rechromatography (silica gel: 230−400 mesh) to afford the pure GA. As a result, the active fraction of GA was obtained from the solvent system of EtOAc:Hx (2:3). The pure solvent fractions were collected in a preweighed container and quantified GA as 1.28 g/100 g of MSK powder. When TLC of the final fraction was seen under UV light, there was no spot other than at Rf = 0.40, which was the same as that of standard GA. The obtained GA was off-white in color with mp of 262 °C.

3.4. Confirmation of Purified Gallic Acid by NMR and HRMS. The structural confirmation of GA was guided by NMR and mass spectroscopy analysis (Table 3). Owing to the high polarity of GA, DMSO-d_6 was used as the NMR solvent for ^{1}H NMR and ^{13}C NMR spectroscopy. Data are presented as follows: chemical shift δ (ppm), integration, multiplicity (s-singlet and bs-broad singlet), and coupling constant in J (Hz). The detailed NMR spectrum depicted the structure as gallic acid (SI Figure 4(a, b)). The ^{1}H NMR and ^{13}C NMR data of purified GA was in line with those reported in the literature for GA.[57,58]

It was observed that proton peaks appeared at 9.18 ppm (bs, 2H) and 8.84 ppm (bs, 1H), indicating the presence of three phenolic hydroxyl groups, whereas the proton signal at 12.24 ppm (bs, 1H) revealed the confirmation of a carboxyl group. In particular, the sharp proton signal at 6.91 ppm attributed to a singlet suggests the existence of two aromatic protons. The mass of the purified GA was determined by HRMS (Figure 3) in the negative ionization mode as m/z: $[M\text{-}H]^-$ calculated: 169.0131 and found: 169.0137 with the score value of 96.65.

3.5. Antioxidant Activity of Purified Gallic Acid. The DPPH radical-scavenging activity of purified GA was compared with standard GA, quercetin, and rutin, and the IC_{50} values were found to be 1.96, 1.03, 18.61, and 13.63 μg/mL, respectively (SI Figure 5). These results are in line with reported data,[59,60] which justifies the superiority of GA as a strong radical scavenger. Brand-Williams et al.[61] reported the highest antiradical activity of GA with a stoichiometry of 4 reduced DPPH molecules per molecule of GA.

Furthermore, the superiority of GA as an antioxidant compared to other polyphenols, such as pyrogallol, methyl gallate, α-tocopherol, and chlorogenic acid, is supported by Rafiee et al.,[16] Asnaashari et al.,[62] and Cheel et al.[63] The probable reason for variation of antioxidant activity among different polyphenols might be the increased stability of the phenoxy radicals, which depends on the number of electron donating hydroxy and methoxy groups.[62] Hence, the study undertaken explored that gallic acid, with three hydroxyl and one carboxylic acid groups, was observed to be the most active as compared to quercetin and rutin.

3.6. Molecular Docking Studies of Major Polyphenols of MSK against SARS CoV-2 M^{pro}. The previous literature has reported an antimalarial drug as a good inhibitor toward the active site of M^{pro}.[64] Among the recommended drugs, hydroxychloroquine has been used in the present study as a

https://doi.org/10.1021/acsfoodscitech.1c00179
ACS Food Sci. Technol. XXXX, XXX, XXX−XXX

control for inhibiting M^{pro} (Figure 4). Hydroxychloroquine has interacted with THR 190, GLN 192, MET 49, GLU 166, PHE 140, LEU 141, SER 144, GLY 143, ASN 142, CYS 145, HIS 163, HIS 164, ASP 187, VAL 186, MET 165, ARG 188, HIS 41, and GLN 189 (SI Figure 6). Simultaneously, the cocrystal ligand α-ketoamide (O6K) was docked at the active site residues of M^{pro} of SARS-CoV-2.

The interacting amino acids include VAL 42, THR 25, HIS 41, LEU 27, HIS 163, LEU 141, ASN 142, GLU 166, HIS 172, SER 144, CYS 145, GLY 143, PHE 140, MET 165, ASP 187, MET 49, and CYS 44, exhibiting a docking score of −6.07 kcal/mol. Seven major polyphenols of MKP underwent molecular docking, and the study revealed that some of the mango polyphenols such as mangiferin, epicatechin, and quercetin have shown effective docking scores of −6.49, −7.23, and −6.52 kcal/mol, respectively (SI Table 2). The docking scores of these three polyphenols are comparable with hydroxychloroquine. Mangiferin complex with M^{pro} of SARS-CoV-2 was stabilized by MET 49, HIS 41, CYS 145, LEU 27, SER 144, PHE 140, LEU 141, ASN 142, GLY 143, HIS 163, MET 165, ARG 188, THR 190, GLN 189, GLN 192, GLU 166, PRO 168, and LEU 167. Epicatechin interacted with HIS 172, SER 144, HIS 163, PHE 140, PRO 168, CYS 145, GLU 166, MET 165, LEU 167, ARG 188, VAL 186, GLN 192, THR 190, GLN 189, HIS 164, MET 49, HIS 41, ASN 142, GLY 143, and LEU 141. The amino acids such as CYS 44, ARG 188, GLN 189, GLU 166, HIS 172, CYS 145, HIS 163, PHE 140, LEU 141, TYR 118, ASN 142, SER 144, GLY 143, MET 65, HIS 164, HIS 41, and MET 49 interacted with the quercetin M^{pro} complex. From the amino acid interactions, it can be seen that all three polyphenols were capable of binding to the catalytic dyad of HIS 41 and CYS145 of M^{pro}. Interestingly, the molecular docking investigation explored that, among seven major polyphenols, three showed good binding affinities. Furthermore, the *in vitro* and *in vivo* investigation of these proposed compounds needs to be done for validation.

The study undertaken revealed that the mango kernel is a rich source of natural antioxidants, which have a tendency to replace artificial ones. All four cultivars studied during this investigation had significant nutritional value including minerals, and the morphology expressed the presence of irregularly shaped particles. On the basis of characterization, Dashehari was considered superior to all other cultivars and was selected for the identification of bioactive compounds by LC-MS/MS, which tentatively screened 50 bioactive compounds based on their MS fragmentation patterns. The separation and purification process of antioxidant-rich gallic acid using column chromatography has been successfully developed in this study. The antioxidant activity of GA proposes its use as a natural antioxidant. Molecular docking studies revealed that three polyphenolic compounds, viz., mangiferin, epicatechin, and quercetin, exhibited effective docking scores along with good binding affinities.

■ ASSOCIATED CONTENT

Supporting Information

The Supporting Information is available free of charge at https://pubs.acs.org/doi/10.1021/acsfoodscitech.1c00179.

Table 1. Mineral composition of cryo-ground MSKP from different cultivars (n = 4). Table 2. Molecular docking for the of docked mango kernel polyphenols with SARS-CoV-2 M^{pro}. Figure 1. LC-MS/MS Chromatogram of mango seed kernel extract in positive ionization mode. Figure 2. Fragmentation pattern (LC-MS/MS) of purified gallic acid. Figure 3. (a) Column Chromatography of mango seed kernel extract; (b) Different impure fractions on TLC plate under UV light; (c) Purified gallic acid compared with standard compound on TLC plate under UV light. Figure 4. (a) ^{1}H NMR (600 MHz, DMSO d_6) δ 12.24 (s, 2H), 9.18 (s, 4H), 8.84 (s, 2H), 6.91 (s, 3H); (b) ^{13}C NMR (151 MHz, DMSO) δ 167.84, 145.77, 138.35, 120.80, 109.07. Figure 5. Two D ligand interaction diagram showing the interactions of (A1), Hydroxychloroquine; (B1), epicatechin; (C1), mangiferin; (D1), quercetin and active site residues of M^{pro} (PDF)

■ AUTHOR INFORMATION

Corresponding Author

Bhupinder Kaur − *Agricultural and Food Engineering Department, Indian Institute of Technology Kharagpur, Kharagpur, West Bengal 721302, India;* orcid.org/0000-0002-4637-8020; Phone: +91-9547484984; Email: bhupisangra@gmail.com, bhupisangra@iitkgp.ac.in

Authors

Himadri Sekhar Maity − *Department of Chemistry, Indian Institute of Technology Kharagpur, Kharagpur, West Bengal 721302, India*

Madhulekha Rakshit − *Agricultural and Food Engineering Department, Indian Institute of Technology Kharagpur, Kharagpur, West Bengal 721302, India*

Prem Prakash Srivastav − *Agricultural and Food Engineering Department, Indian Institute of Technology Kharagpur, Kharagpur, West Bengal 721302, India*

Ahindra Nag − *Department of Chemistry, Indian Institute of Technology Kharagpur, Kharagpur, West Bengal 721302, India*

Complete contact information is available at: https://pubs.acs.org/10.1021/acsfoodscitech.1c00179

Notes

The authors declare no competing financial interest.

■ ACKNOWLEDGMENTS

We would like to thank Science and Technology Entrepreneurs Park (STEP), IIT Kharagpur, West Bengal, India, for providing the byproducts of mango.

■ ABBREVIATIONS USED

MKP, mango kernel powder; MKE, mango kernel extract; GA, gallic acid; ^{1}H, proton; ^{13}C, natural, stable isotope of carbon with six protons and seven neutrons; m/z, mass-to-charge ratio; SD, standard deviation; δ, chemical shift (ppm)

■ REFERENCES

(1) Duque-Acevedo, M.; Belmonte-Ureña, L. J.; Cortés-García, F. J.; Camacho-Ferre, F. Agricultural waste: Review of the evolution, approaches and perspectives on alternative uses. *Global Ecology and Conservation* **2020**, *22*, e00902.

(2) Ravani, A.; Joshi, D. C. Mango and it's by product utilization − a review. *Trends Post Harvest Technol.* **2013**, *1* (1), 55−67.

(3) Leyva-López, N.; Lizárraga-Velázquez, C. E.; Hernández, C.; Sánchez-Gutiérrez, E. Y. Exploitation of Agro-Industrial Waste as Potential Source of Bioactive Compounds for Aquaculture. *Foods* **2020**, *9*, 843.

(4) Dorta, E.; Lobo, M. G.; González, M. Using drying treatments to stabilise mango peel and seed: Effect on antioxidant activity. *LWT - Food Sci. Technol.* **2012**, *45* (2), 261−268.
(5) Yang, L.; Xiao, X.; Gu, K. Agricultural Waste Recycling Optimization of Family Farms Based on Environmental Management Accounting in Rural China. *Sustainability* **2021**, *13*, 5515.
(6) Romelle, F. D.; Rani, A.; Manohar; Rcrc, S. Chemical composition of some selected fruit peels. *European Journal of Food Science and Technology* **2016**, *4* (4), 12−21.
(7) Kaur, B.; Srivastav, P. P. Effect of Cryogenic grinding on chemical and morphological characteristics of mango (Mangifera indica L.) peel powder. *J. Food Process. Preserv.* **2018**, *42* (4), e13583.
(8) Bandyopadhyay, K.; Chakraborty, C.; Bhattacharyya, S. Fortification of Mango Peel and Kernel Powder in Cookies Formulation. *Journal of Academia and Industrial Research* **2014**, *2* (12), 661−664.
(9) National Horticulture Board. Horticultural statistics at a glance 2017−2018. http://nhb.gov.in/statistics/Publication/Horticulture%20Statistics%20at%20a%20Glance-2018.pdf (accessed 2019−07−14).
(10) Yatnatti, S.; Vijayalakshmi, D.; Chandru, R. Processing and nutritive value of mango seed kernel flour. *Current Research in Nutrition and Food Science* **2014**, *2* (3), 170−175.
(11) Navarro, M.; Arnaez, E.; Moreira, I.; Quesada, S.; Azofeifa, G.; Wilhelm, K.; Vargas, F.; Chen, P. Polyphenolic Characterization, Antioxidant, and Cytotoxic Activities of *Mangifera indica* Cultivars from Costa Rica. *Foods* **2019**, *8* (9), 384.
(12) Gómez-Caravaca, A. M.; López-Cobo, A.; Verardo, V.; Segura-Carretero, A.; Fernández-Gutiérrez, A. HPLC-DAD-q-TOF-MS as a powerful platform for the determination of phenolic and other polar compounds in the edible part of mango and its by-products (peel, seed, and seed husk). *Electrophoresis* **2016**, *37* (7−8), 1072−1084.
(13) Rocha Ribeiro, S. M.; Queiroz, J. H.; Lopes Ribeiro de Queiroz, M. E.; Campos, F. M.; Pinheiro Sant'Ana, H. M. Antioxidant in mango (Mangifera indica L.) pulp. *Plant Foods Hum. Nutr.* **2007**, *62* (1), 13−17.
(14) Soong, Y. Y.; Barlow, P. J. Antioxidant activity and phenolic content of selected fruit seeds. *Food Chem.* **2004**, *88* (3), 411−417.
(15) Mwaurah, P. W.; Kumar, S.; Kumar, N.; Panghal, A.; Attkan, A. K.; Singh, V. K.; Garg, M. K. Physicochemical characteristics, bioactive compounds and industrial applications of mango kernel and its products: A review. *Compr. Rev. Food Sci. Food Saf.* **2020**, *19* (5), 2421−2446.
(16) Velderrain-Rodríguez, G. R.; Torres-Moreno, H.; Villegas-Ochoa, M. A.; Ayala-Zavala, J. F.; Robles-Zepeda, R. E.; Wall-Medrano, A.; González-Aguilar, G. A. Gallic Acid Content and an Antioxidant Mechanism Are Responsible for the Antiproliferative Activity of 'Ataulfo' Mango Peel on LS180 Cells. *Molecules* **2018**, *23* (3), 695.
(17) Ediriweera, M. K.; Tennekoon, K. H.; Samarakoon, S. R. A Review on Ethnopharmacological Applications, Pharmacological Activities and Bioactive Compounds of *Mangifera indica* (Mango). *Evidence-based complementary and alternative medicine* **2017**, *2017*, 1.
(18) Abri, A.; Maleki, M. Isolation and identification of gallic acid from the elaeagnus angustifolia leaves and determination of total phenolic, flavonoids contents and investigation of antioxidant activity. *Quarterly Journal of Iranian Chemical Communication* **2016**, *4* (2), 146−154.
(19) Yang, K.; Zhang, L.; Liao, P.; Xiao, Z.; Zhang, F.; Sindaye, D.; Xin, Z.; Tan, C.; Deng, J.; Yin, Y.; Deng. Impact of Gallic Acid on Gut Health: Focus on the Gut Microbiome, Immune Response, and Mechanisms of Action. *Front. Immunol.* **2020**, *11*, 2231.
(20) Bai, J.; Zhang, Y.; Tang, C.; Hou, Y.; Ai, X.; Chen, X.; Zhang, Y.; Wang, X.; Meng, X. Gallic acid: Pharmacological activities and molecular mechanisms involved in inflammation-related diseases. *Biomed. Pharmacother.* **2021**, *133*, 110985.
(21) Kim, M. J.; Seong, A. R.; Yoo, J. Y.; Jin, C. H.; Lee, Y. H.; Kim, Y. J.; Lee, J.; Jun, W. J.; Yoon, H. G. Gallic acid, a histone acetyltransferase inhibitor, suppresses β-amyloid neurotoxicity by inhibiting microglial-mediated neuroinflammation. *Mol. Nutr. Food Res.* **2011**, *55* (12), 1798−1808.
(22) García-Rivera, D.; Delgado, R.; Bougarne, N.; Haegeman, G.; Berghe, W. V. Gallic acid indanone and mangiferin xanthone are strong determinants of immunosuppressive anti-tumour effects of Mangifera indica L. bark in MDA-MB231 breast cancer cells. *Cancer Lett.* **2011**, *305* (1), 21−31.
(23) Choi, K. C.; Lee, Y. H.; Jung, M. G.; Kwon, S. H.; Kim, M. J.; Jun, W. J.; Lee, J.; Lee, J. M.; Yoon, H. G. Gallic acid suppresses lipopolysaccharide-induced nuclear factor-kappaB signaling by preventing RelA acetylation in A549 lung cancer cells. *Mol. Cancer Res.* **2009**, *7* (12), 2011−2021.
(24) Jin, Z.; Du, X.; Xu, Y.; et al. Structure of Mpro from SARS-CoV-2 and discovery of its inhibitors. *Nature* **2020**, *582*, 289−293.
(25) Rut, W.; Groborz, K.; Zhang, L.; et al. SARS-CoV-2 Mpro inhibitors and activity-based probes for patient-sample imaging. *Nat. Chem. Biol.* **2021**, *17*, 222−228.
(26) Sobhia, M. E.; Ghosh, K.; Sivangula, S.; Kumar, S.; Singh, H. Identification of potential SARS-CoV-2 Mpro inhibitors integrating molecular docking and water thermodynamics. *J. Biomol. Struct. Dyn.* **2021**, 1−11.
(27) Mengist, H. M.; Dilnessa, T.; Jin, T. Structural Basis of Potential Inhibitors Targeting SARS-CoV-2 Main Protease. *Front. Chem.* **2021**, *9*, 7.
(28) Morris, G. M.; Lim-Wilby, M. Molecular docking. *Methods Mol. Biol.* **2008**, *443*, 365−382.
(29) Ghodki, B. M.; Goswami, T. K. Effect of grinding temperatures on particle and physicochemical characteristics of black pepper powder. *Powder Technol.* **2016**, *299*, 168−177.
(30) Réblová, Z. Effect of temperature on the antioxidant activity of phenolic acids. *Czech J. Food Sci.* **2012**, *30* (2), 171−177.
(31) Kaur, B.; Pyne, S. K.; Srivastav, P. P.; Nag, A. Characterization and comparison of mango (Mangifera indica) processing waste from five Indian cultivars. *Int. J. Chem. Stud.* **2019**, *7* (4), 2844−2849.
(32) Abdullah, A. H.; Mirghani, M. E. S.; Jamal, P. Antibacterial activity of Malaysian mango kernel. *Afr. J. Biotechnol.* **2011**, *10* (81), 18739−18748.
(33) Mirghani, M. E. S.; Yosuf, F.; Kabbashi, N. A.; Vejaya, J.; Yousuf, Z. B. M. Antibacterial Activity of Mango Kernel Extracts. *J. Appl. Sci.* **2009**, *9* (17), 3013−3019.
(34) Abdalla, A. E. M.; Darwish, S. M.; Ayad, E. H. E.; El-Hamahmy, R. M. Egyptian mango by-product 2: Antioxidant and antimicrobial activities of extract and oil from mango seed kernel. *Food Chem.* **2007**, *103* (4), 1141−1152.
(35) Ashoush, I. S.; Gadallah, M. G. E. Utilization of Mango Peels and Seed Kernels Powders as Sources of Phytochemicals in Biscuit. *World J. Dairy Food Sci.* **2011**, *6* (1), 35−42.
(36) Torres-León, C.; Rojas, R.; Serna-Cock, L.; Belmares-Cerda, R.; Aguilar, C. N. Extraction of antioxidants from mango seed kernel: Optimization assisted by microwave. *Food Bioprod. Process.* **2017**, *105*, 188−196.
(37) AOAC. *Official Methods of Analysis*, 16th ed.; Association of Official Analytical Chemists: Washington, DC, USA, 2004.
(38) Ramirez, J. E.; Zambrano, R.; Sepúlveda, B.; Simirgiotis, M. J. Antioxidant properties and hyphenated HPLC-PDA-MS profiling of chilean pica mango fruits (Mangifera indica L. Cv. piqueño). *Molecules* **2014**, *19* (1), 438−458.
(39) Gauri, S. S.; Mandal, S. M.; Dey, S.; Pati, B. R. Biotransformation of p-coumaric acid and 2,4-dichlorophenoxy acetic acid by Azotobacter sp. strain SSB81. *Bioresour. Technol.* **2012**, *126*, 350−353.
(40) Alavi Rafiee, S.; Farhoosh, R.; Sharif, A. Antioxidant Activity of Gallic Acid as Affected by an Extra Carboxyl Group than Pyrogallol in Various Oxidative Environments. *Eur. J. Lipid Sci. Technol.* **2018**, *120*, 1800319.
(41) Jin, Z.; Du, X.; Xu, Y.; Deng, Y.; Liu, M.; Zhao, Y.; Zhang, B.; Li, X.; Zhang, L.; Peng, C.; Duan, Y.; Yu, J.; Wang, L.; Yang, K.; Liu, F.; Jiang, R.; Yang, X.; You, T.; Liu, X.; Yang, H. Structure of M^{pro} from COVID-19 virus and discovery of its inhibitors. *Nature* **2020**, *582*, 289−293.

https://doi.org/10.1021/acsfoodscitech.1c00179
ACS Food Sci. Technol. XXXX, XXX, XXX−XXX

(42) Ajila, C. M.; Rao, U. J. S. P. Mango peel dietary fibre: Composition and associated bound phenolics. *J. Funct. Foods* **2013**, *5* (1), 444−450.
(43) Tunchaiyaphum, S.; Eshtiaghi, M. N.; Yoswathana, N. Extraction of Bioactive Compounds from Mango Peels Using Green Technology. *Int. J. Chem. Eng. Appl.* **2013**, *4* (4), 194−198.
(44) Muhamad, S. A. S.; Jamilah, B.; Russly, A. R.; Faridah, A. The antibacterial activities and chemical composition of extracts from Carica papaya cv. Sekaki/Hong Kong seed. *Int. Food Res. J.* **2017**, *24* (2), 810−818.
(45) Maisuthisakul, P. Antioxidant Potential and Phenolic Constituents of Mango Seed Kernel from Various Extraction Methods. *Kasetsart J. (Nat. Sci)* **2009**, *43*, 290−297.
(46) Lv, G.; Zhang, Z.; Pan, H.; Fan, L. Effect of Physical Modification of Mushroom (A. chaxingashu) Powders on their Physical and Chemical Properties. *Food Sci. Technol. Res.* **2014**, *20* (4), 731−738.
(47) Leghari, M. H.; Sheikh, S. A.; Kumbhar, M. B.; Baloch, A. F. Mineral Content in Dehydrated Mango Powder. *J. Basic Appl. Sci.* **2013**, *9*, 21−25.
(48) Oniszczuk, A.; Olech, M. Optimization of ultrasound-assisted extraction and LC-ESI-MS/MS analysis of phenolic acids from Brassica oleracea L. var. sabellica. *Ind. Crops Prod.* **2016**, *83*, 359−363.
(49) Kumar, S.; Singh, A.; Kumar, B. Identification and characterization of phenolics and terpenoids from ethanolic extracts of Phyllanthus species by HPLC-ESI-QTOF-MS/MS. *J. Pharm. Anal.* **2017**, *7* (4), 214−222.
(50) Rameshkumar, A.; Sivasudha, T.; Jeyadevi, R.; Sangeetha, B.; Aseervatham, G. S. M.; Maheshwari, M. Profiling of phenolic compounds using UPLC-Q-TOF-MS/MS and nephroprotective activity of Indian green leafy vegetable Merremia emarginata (Burm. f.). *Food Res. Int.* **2013**, *50* (1), 94−101.
(51) Catarino, M. D.; Silva, A. M. S.; Saraiva, S. C.; Sobral, A. J. F. N.; Cardoso, S. M. Characterization of phenolic constituents and evaluation of antioxidant properties of leaves and stems of Eriocephalus africanus. *Arabian J. Chem.* **2018**, *11* (1), 62−69.
(52) Kumar, S.; Chandra, P.; Bajpai, V.; Singh, A.; Srivastava, M.; Mishra, D. K.; Kumar, B. Rapid qualitative and quantitative analysis of bioactive compounds from Phyllanthus amarus using LC/MS/MS techniques. *Ind. Crops Prod.* **2015**, *69*, 143−152.
(53) Abu-Reidah, I. M.; Ali-Shtayeh, M. S.; Jamous, R. M.; Arráez-Román, D.; Segura-Carretero, A. HPLC-DAD-ESI-MS/MS screening of bioactive components from Rhus coriaria L. (Sumac) fruits. *Food Chem.* **2015**, *166*, 179−191.
(54) Ola, S. S.; Catia, G.; Marzia, I.; Francesco, V. F.; Afolabi, A. A.; Nadia, M. HPLC/DAD/MS characterisation and analysis of flavonoids and cynnamoil derivatives in four Nigerian green-leafy vegetables. *Food Chem.* **2009**, *115* (4), 1568−1574.
(55) Yang, B.; Kortesniemi, M.; Liu, P.; Karonen, M.; Salminen, J. P. Analysis of hydrolyzable tannins and other phenolic compounds in emblic leafflower (Phyllanthus emblica L.) fruits by high performance liquid chromatography-electrospray ionization mass spectrometry. *J. Agric. Food Chem.* **2012**, *60* (35), 8672−8683.
(56) Wyrepkowski, C. C.; Gomes da Costa, D. L. M.; Sinhorin, A. P.; Vilegas, W.; De Grandis, R. A.; Resende, F. A.; Varanda, E. A.; Dos Santos, L. C. Characterization and quantification of the compounds of the ethanolic extract from caesalpinia ferrea stem bark and evaluation of their mutagenic activity. *Molecules* **2014**, *19* (10), 16039−16057.
(57) López-Martínez, L. M.; Santacruz-Ortega, H.; Navarro, R. E.; Sotelo-Mundo, R. R.; González-Aguilar, G. A. A ^{1}H NMR investigation of the interaction between phenolic acids found in mango (Manguifera indica cv Ataulfo) and papaya (Carica papaya cv Maradol) and 1,1-diphenyl-2-picrylhydrazyl (DPPH) free radicals. *PLoS One* **2015**, *10* (11), e0140242.
(58) Kamatham, S.; Kumar, N.; Gudipalli, P. Isolation and characterization of gallic acid and methyl gallate from the seed coats of Givotia rottleriformis Griff. and their anti-proliferative effect on human epidermoid carcinoma A431 cells. *Toxicol Reports* **2015**, *2*, 520−529.
(59) Rusmana, D.; Wahyudianingsih, R.; Elisabeth, M.; Balqis; Maesaroh; Widowati, W. Antioxidant activity of Phyllanthus niruri extract, rutin and quercetin. *Indonesian Biomedical Journal* **2017**, *9* (2), 84−90.
(60) Karamac, M.; Kosinska, A.; Pegg, R. Comparison of radical-scavenging activities for selected phenolic acids. *Polish J. Food Nutr. Sci.* **2005**, *14* (2), 165−169.
(61) Brand-Williams, W.; Cuvelier, M. E.; Berset, C. Use of a Free Radical Method to Evaluate Antioxidant Activity. *Leb Wiss Technol.* **1995**, *28*, 25−30.
(62) Asnaashari, M.; Farhoosh, R.; Sharif, A. Antioxidant activity of gallic acid and methyl gallate in triacylglycerols of Kilka fish oil and its oil-in-water emulsion. *Food Chem.* **2014**, *159*, 439−444.
(63) Cheel, J.; Schmeda-Hirschmann, G.; Jordan, M.; Theoduloz, C.; Rodríguez, J. A.; Gerth, A.; Wilken, D. Free radical scavenging activity and secondary metabolites from in vitro cultures of Sanicula graveolens. *Z. Naturforsch., C: J. Biosci.* **2007**, *62* (7−8), 555−562.
(64) Ong, W. Y.; Go, M. L.; Wang, D. Y.; Cheah, I. K. M.; Halliwell, B. Effects of antimalarial drugs on neuroinflammation-potential use for treatment of COVID-19-related neurologic complications. *Mol. Neurobiol.* **2021**, *58* (1), 106−117.

https://doi.org/10.1021/acsfoodscitech.1c00179
ACS Food Sci. Technol. XXXX, XXX, XXX−XXX